

An SEIHR model with age group and social contact for analysis of Fuzhou COVID-19 large wave

Xiaomin Lan ^{a,1}, Guangmin Chen ^{b,1}, Ruiyang Zhou ^a, Kuicheng Zheng ^b,
Shaojian Cai ^b, Fengying Wei ^{a,c,d,*}, Zhen Jin ^{e,**}, Xuerong Mao ^{f,***}

^a School of Mathematics and Statistics, Fuzhou University, Fuzhou, 350116, Fujian, China

^b Fujian Provincial Center for Disease Control and Prevention, Fuzhou, 350012, Fujian, China

^c Center for Applied Mathematics of Fujian Province, Fuzhou, 350116, Fujian, China

^d Key Laboratory of Operations Research and Control of Universities in Fujian, Fuzhou University, Fuzhou, 350116, Fujian, China

^e Complex Models Research Center, Shanxi University, Taiyuan, 030006, Shanxi, China

^f Department of Mathematics and Statistics, University of Strathclyde, Glasgow, G1 1XH, UK

ARTICLE INFO

Article history:

Received 17 October 2023

Received in revised form 22 March 2024

Accepted 8 April 2024

Handling Editor: Dr Yijun Lou

Keywords:

COVID-19 model

Age group

Omicron BA.5.2 variant

Contact matrix

Social contact

ABSTRACT

Background: The structure of age groups and social contacts of the total population influenced infection scales and hospital-bed requirements, especially influenced severe infections and deaths during the global prevalence of COVID-19. Before the end of the year 2022, Chinese government implemented the national vaccination and had built the herd immunity cross the country, and announced Twenty Measures (November 11) and Ten New Measures (December 7) for further modifications of dynamic zero-COVID polity on the Chinese mainland. With the nation-wide vaccination and modified measures background, Fuzhou COVID-19 large wave (November 19, 2022–February 9, 2023) led by Omicron BA.5.2 variant was recorded and prevailed for three months in Fujian Province.

Methods: A multi-age groups susceptible-exposed-infected-hospitalized-recovered (SEIHR) COVID-19 model with social contacts was proposed in this study. The main object was to evaluate the impacts of age groups and social contacts of the total population. The idea of Least Squares method was governed to perform the data fittings of four age groups against the surveillance data from Fujian Provincial Center for Disease Control and Prevention (Fujian CDC). The next generation matrix method was used to compute basic reproduction number for the total population and for the specific age group. The tendencies of effective reproduction number of four age groups were plotted by using the Epiestim R package and the SEIHR model for in-depth discussions. The sensitivity analysis by using sensitivity index and partial rank correlation coefficients values (PRCC values) were operated to reveal the differences of age groups against the main parameters.

Results: The main epidemiological features such as basic reproduction number, effective reproduction number and sensitivity analysis were extensively discussed for multi-age groups SEIHR model in this study. Firstly, by using of the next generation matrix method, basic reproduction number R_0 of the total population was estimated as 1.57 using parameter values of four age groups of Fuzhou COVID-19 large wave. Given age group k , the values of R_{0k} (age group k to age group k), the values of R_0^k (an infected of age group k to

* Corresponding author. School of Mathematics and Statistics, Fuzhou University, Fuzhou, 350116, Fujian, China.

** Corresponding author.

*** Corresponding author.

E-mail addresses: weifengying@fzu.edu.cn (F. Wei), jinzhn@263.net (Z. Jin), x.mao@strath.ac.uk (X. Mao).

Peer review under responsibility of KeAi Communications Co., Ltd.

¹ These authors contributed equally to this work.

the total population) and the values of R_0^k (an infected of the total population to age group k) were also estimated, in which the explorations of the impacts of age groups revealed that the relationship $R_0^k > R_{0k} > \bar{R}_0^k$ was valid. Then, the fluctuating tendencies of effective reproduction number R_t were demonstrated by using two approaches (the surveillance data and the SEIHR model) for Fuzhou COVID-19 large wave, during which high-risk group (G4 group) mainly contributed the infection scale due to high susceptibility to infection and high risks to basic diseases. Further, the sensitivity analysis using two approaches (the sensitivity index and the PRCC values) revealed that susceptibility to infection of age groups played the vital roles, while the numerical simulation showed that infection scale varied with the changes of social contacts of age groups. The results of this study claimed that the high-risk group out of the total population was concerned by the local government with the highest susceptibility to infection against COVID-19.

Conclusions: This study verified that the partition structure of age groups of the total population, the susceptibility to infection of age groups, the social contacts among age groups were the important contributors of infection scale. The less social contacts and adequate hospital beds for high-risk group were profitable to control the spread of COVID-19. To avoid the emergence of medical runs against new variant in the future, the policymakers from local government were suggested to decline social contacts when hospital beds were limited.

© 2024 The Authors. Publishing services by Elsevier B.V. on behalf of KeAi Communications Co. Ltd. This is an open access article under the CC BY-NC-ND license (<http://creativecommons.org/licenses/by-nc-nd/4.0/>).

1. Introduction

The first COVID-19 epidemic caused by SARS-CoV-2 Omicron variant was recorded in December of 2021 at Tianjin City (Tan et al., 2022) since dynamic zero-COVID policy was carried out in August of 2021 (Liang et al., 2022). Afterwards, the COVID-19 epidemics were contained on the Chinese mainland until the implements of Twenty Measures and Ten New Measures as of the end of 2022 (Chen et al., 2022; Wei et al., 2023; Zeng et al., 2023; Zhong et al., 2022). The COVID-19 epidemics led by SARS-CoV-2 Omicron variant in Fujian Province included Quanzhou epidemic (March 10–April 14, 2022), Xiapu epidemic (July 1–July 15, 2022), Fuzhou COVID-19 small wave (October 22–November 18, 2022) and Fuzhou COVID-19 large wave (November 19, 2022–February 9, 2023). To further optimize the COVID-19 responses before the end of the year 2022, Chinese government announced Twenty Measures on November 11 in (Twenty Measures, 2022; The State Council The People's Republic of China, 2022a), then announced Ten New Measures on December 7 in (Ten New Measures, 2022; The State Council The People's Republic of China, 2022b) against the spreading of COVID-19. More precisely, the eleventh measure of Twenty Measures was to prepare inpatient beds and beds for the severe cases according to their threshold values of COVID-19 nucleic acid tests and their clinic severeness, which meant that all infection cases required the hospital beds before December 7 of the year 2022. The fifth measure of Ten New Measures was to suggest the asymptomatic carriers and those with mild symptoms undergoing home quarantine, the close contacts undergoing five days of home quarantine, which meant that the asymptomatic cases or those with mild symptoms did not require the hospital beds after December 7 of the year 2022. These differences of the hospital-bed requirements for infection cases were very significant to the policymaker of the local government.

Meanwhile, the vaccination situation for the Chinese mainland was in high-level in (Zhou et al., 2024), which was reported by the key media that 1272.83 (90.28%) million individuals on the Chinese mainland finished the full vaccination as of November 28 of the year 2022 in (People's Daily Online, 2023). Especially, the vaccination situation of Fujian Province had been improved during the period from November 1 to December 20 of the year 2022 as shown in Fig. 1, from which the total number of the full vaccination ranged from 39.0028 (93.90%) to 39.0749 (94.10%) million individuals, the total number of the boosted vaccination ranged from 24.2605 to 24.6716 million individuals, the cumulative number of the vaccination ranged from 102.1986 to 103.0916 doses (Health Commission of Fujian Province, 2022a,b). The high coverage situation of the vaccine in Fujian Province implied that the number of the individuals who were not been vaccinated was very less, which also reflected that the herd immunity of the total population was established. Based on the vaccination situation, aiming at optimizing the COVID-19 responses, the managers from Fujian Provincial Center for Disease Control and Prevention (i.e., Fujian CDC) collected the surveillance data of COVID-19 from the healthcare institutions and medical agents, then they reported to the policymakers of the local government for optimizing further measures against COVID-19.

The SEIR-type compartment models and the models alike were usually governed to investigate the epidemiological characteristics and dynamic behaviors of infectious diseases. The recent studies combining the multi-age groups and the hospitalization data in (Kimathi et al., 2021; Lu et al., 2019; Zhou et al., 2019; Li et al., 2022; Makhoul et al., 2021; Liu & Wei, 2022; Wei & Xue, 2020; Yu et al., 2023; Zhang & Wei, 2020; Wei et al., 2021; Zhai et al., 2023; Taboe et al., 2022; Wei et al., 2023; Wu & Feng, 2024), were less. For instance, the studies for two-age groups compartment model in (Taboe et al., 2022) indicated that the individuals under 65 years old were the primary drivers of the COVID-19 pandemic in West Africa. The findings in (Wei et al., 2023) showed that two-age groups compartment model with non-pharmaceutical interventions described the successful containment of the Shijiazhuang epidemic. The results of (Wu & Feng, 2024) showed that the

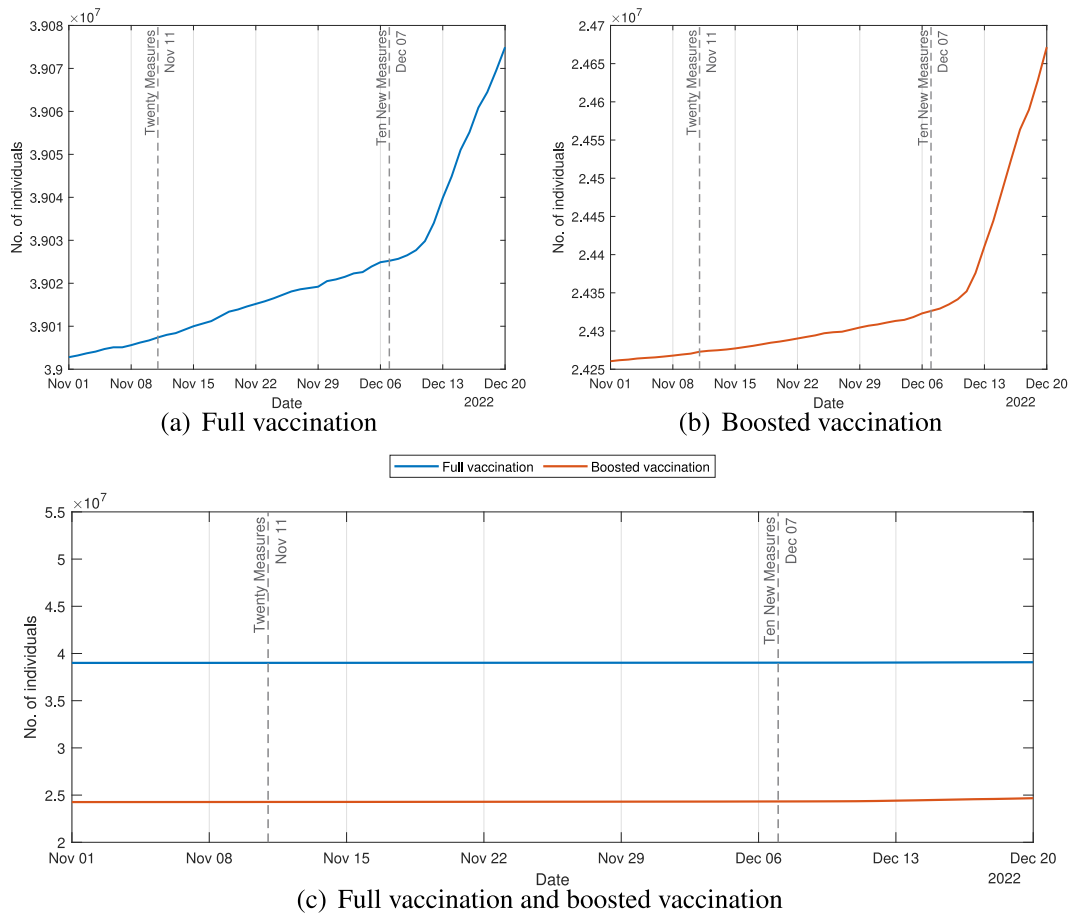


Fig. 1. Vaccination situation of Fujian Province from November 1 to December 20 of the year 2022 against COVID-19. Full vaccination (Left top) and booster vaccination (Right top) are presented respectively. Vaccination situation of Fujian Province with the same scale-magnitude (Bottom).

threshold dynamics of COVID-19 transmission relied on infection age and spatial diffusion of a space-age structured model. To analyze the main epidemiological features of Fuzhou COVID-19 large wave, we established an SEIHR compartment model and studied the impacts of the heterogeneity for social contacts and age groups of the total population, in which the requirements on hospital-beds were mainly for severe cases and those with symptoms, the asymptomatic cases and the mild/moderate cases instead. The multi-age groups SEIHR model of this study filled in the gap of the compartment models with hospital-bed requirements in the existed contributions. The main results of this study would provide the valuable insights for the managers of Fujian CDC and the policymakers of the local government.

2. Methods

2.1. Definition of the hospitalized case

The standards for identifying the hospitalized cases were referred as the cases who were diagnosed in hospitals and then were discharged from hospitals due to their recoveries by the surveillance data from Fujian Provincial Center for Disease Control and Prevention (i.e., Fujian CDC). Here, the hospitalized cases were not all symptomatic infections as explored in the recent contributions (Chen et al., 2022; Wei et al., 2022).

2.2. Data sources and contact matrix

2.2.1. Surveillance data and collection

The surveillance data of this study were recorded by Fujian CDC. The funder of the study had no role in study design, data collection and analysis, interpretation and writing of the report. The corresponding authors had full access to all data in the study and had final responsibility for the decision to submit for publication. The total population was separated into four

parts: G1 group (infants and school-oriented children, 0–11 years old), G2 group (school-oriented teenagers, 12–19 years old), G3 group (job-oriented young adults, 20–59 years old), G4 group (home-oriented elder adults, 60 years old and over), in which G4 group took high risks during the prevalence of COVID-19 due to their basic diseases such as diabetes, high blood pressure, heart disease, hyperlipidemia and chronic inflammation.

The surveillance data showed that Fuzhou COVID-19 small wave brought 1,529 infection cases during the implements of Twenty Measures on November 11; Fuzhou COVID-19 large wave brought 74,528 infection cases during the implements of Ten New Measures on December 7. These two waves were caused by SARS-CoV-2 Omicron BA.5.2 variant, but the hospitalized requirements from Fuzhou COVID-19 large wave clearly changed before and after December 7. Precisely, the infected cases immediately occupied hospital beds when confirmed before December 7, while the infected cases took several days waiting for hospital beds when confirmed due to inadequate beds against COVID-19 after December 7. Therefore, we separated surveillance data into the infected cases and the hospitalized cases by four age groups. Here, the infection scale for the hospitalized cases was less than that of the infected cases after December 7, because the asymptomatic cases and those with mild symptoms stayed at home for medical care after onset of illness was detected.

2.2.2. Contact matrix

By the heterogeneous 16×16 contact matrix of the Chinese mainland from (Prem et al., 2021) and the weighted average method, we derived a heterogeneous 4×4 contact matrix describing the average contact numbers of four age groups in Fig. 2 and table 1 in (Lan et al., 2024), in which the computation details of the values for contact matrix were provided in Appendix A. Here, these two contact matrices showed the heterogeneity of social contact patterns among age groups of the total population. Further, we assumed that C_{jk} was not equal to C_{kj} due to their essentially different meanings. Precisely, C_{jk} meant for the daily average number of contacts with the individuals of age group k by an individual of age j ; C_{kj} stood for the daily average number of contacts with the individuals of age group j by an individual of age k , when we fixed the partition of four age groups of the total population in this study.

2.3. Age-group SEIHR model

According to the heterogeneities among age groups of the surveillance data from Fujian CDC, we established a multi-age groups SEIHR model in this study. Precisely, we kept the features of the surveillance data and made the following assumptions in this study. (i) The total population in a given region/city was assumed to remain the constant with the same birth rate and death rate during Fuzhou COVID-19 large wave. (ii) We neglected the fatality rate of COVID-19 of the total population due to the 90-day duration of Fuzhou COVID-19 large wave. (iii) The hospitalized individuals were regarded as stopping the transmission with their good treatments in health care facilities, the hospitalized individuals would transfer into the recovered compartment further returned back the susceptible compartment losing the temporary immunities within next six months in this study. (iv) The contact pattern between the susceptible individuals and the infected individuals was described by the standard incidence rate. (v) The aging rates among age groups were assumed to be the constants. Here, the SEIHR model consisted of the susceptible (S_k , the individuals who were not the hosts of SARS-CoV-2 virus), the exposed (E_k , the individuals who were infected by SARS-CoV-2 virus and started their incubation periods), the infected (I_k , the infectious individuals had no requirements on hospital beds), the hospitalized (H_k , the infectious individuals had requirements on hospital beds) and the recovered (R_k , the individuals who had transient immunities and would return to the susceptible population) of age group k with in the total population $N_k = S_k + E_k + I_k + H_k + R_k$ for $k = 1, 2, \dots, K$. So, the multi-age groups SEIHR model was described as follows:

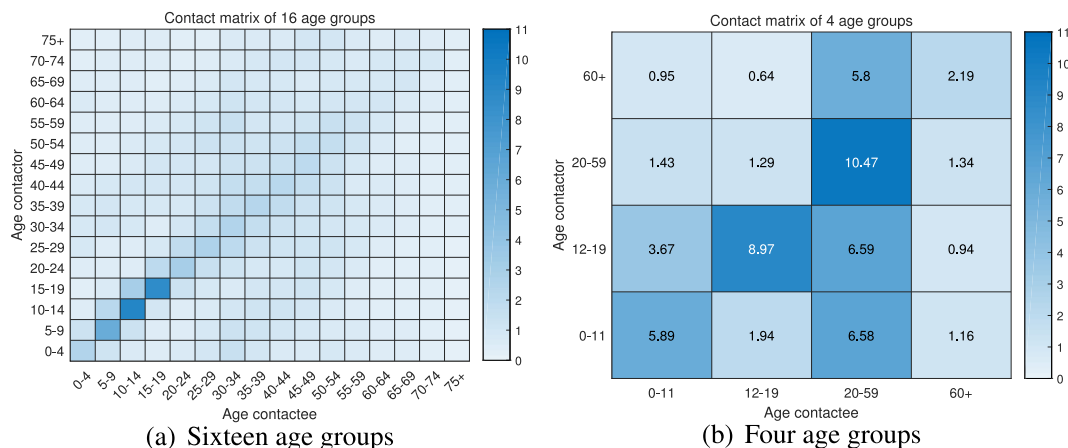


Fig. 2. The heterogeneity of 16×16 contact matrix of the Chinese mainland was given in (Prem et al., 2021) (Left). The heterogeneity of 4×4 contact matrix of the Chinese mainland was computed by using the weighted average method (Right).

$$\begin{aligned}
 \dot{S}_k(t) &= \mu\delta_{k,1}N - \sum_{j=1}^K I_j C_{jk} \frac{S_k}{N_k} \lambda_k + \nu R_k - \mu S_k + \omega_{k-1} S_{k-1} - \omega_k S_k, \\
 \dot{E}_k(t) &= \sum_{j=1}^K I_j C_{jk} \frac{S_k}{N_k} \lambda_k - (\alpha + \mu) E_k + \omega_{k-1} E_{k-1} - \omega_k E_k, \\
 \dot{I}_k(t) &= \alpha E_k - (\gamma_{1k} + \theta_k + \mu) I_k + \omega_{k-1} I_{k-1} - \omega_k I_k, \\
 \dot{H}_k(t) &= \theta_k I_k - (\gamma_{2k} + \mu) H_k + \omega_{k-1} H_{k-1} - \omega_k H_k, \\
 \dot{R}_k(t) &= \gamma_{1k} I_k + \gamma_{2k} H_k - (\nu + \mu) R_k + \omega_{k-1} R_{k-1} - \omega_k R_k,
 \end{aligned} \tag{1}$$

where $\delta_{1,1} = 1$ and $\delta_{k,1} = 0$ for $k \neq 1$, $\omega_0 = 0$ and $\omega_K = 0$. Here, λ_k were the susceptibility to infection of S_k ; C_{jk} , the daily average number of contacts with individuals of age group k by an individual of age group j ; ω_k , the daily aging rate from group k to $k + 1$; γ_{1k} , the average recovery rates of I_k ; γ_{2k} , the average recovery rates of H_k ; θ_k , the average hospitalization rates of age group k ; μ , the natural birth/death rate; $1/\nu$, the average duration of immune protection; $1/\alpha$, the average incubation period.

The initial values of the SEIHR model were set as follows. By the population scale of age groups in 2021 from Fuzhou City Bureau of Statistics (Fuzhou Statistics Bureau, 2020), the initial value of the susceptible was given by $S_k(0) = N_k(0) - E_k(0) - I_k(0) - H_k(0) - R_k(0)$, the initial value of the exposed $E_k(0)$ was set by Fuzhou Health Care Commission (Fuzhou Health Commission, 2023). Here, the initial values of the infected $I_k(0)$ and the hospitalized $H_k(0)$ were supposed to be zero on November 17 due to the very beginning of Fuzhou COVID-19 large wave. By the report from Fuzhou Health Care Commission (Fuzhou Health Commission, 2023), the initial of the recovered $R_k(0)$ was set to be 1,600 by the recorded cases from Fuzhou COVID-19 small wave and closed-loop management, which was distributed into the initial values of four age groups in Table B.1.

Meanwhile, the parameter values of the SEIHR model were set by steps. Firstly, the awareness delay was assumed to be 2 days for Fuzhou COVID-19 large wave, because Omicron BA.5.2 variant was a highly infectious variant as studied in (Duan & Jin, 2022; Huang et al., 2020; Huo et al., 2023; Nguyen et al., 2021; Xiong et al., 2023; Fuzhou Statistics Bureau, 2020). Then, the average lengths of hospitalization $1/\gamma_{2k}$ were calculated using the surveillance data from Fujian CDC. The main parameter values ω_k , γ_{1k} , μ , $1/\nu$ and $1/\alpha$ were provided in the recent contributions of Table B.2. Further, the hospitalization rates θ_k and susceptibility to infection λ_k were derived by data fittings, in which θ_k took less values after December 7, λ_k took high values before December 3 as presented in Table B.3.

2.4. Basic reproduction number

By next generation matrix method (van den Driessche & Watmough, 2002), the expression of basic reproduction number

$$R_0 = \rho(FV^{-1}) = \rho(-F_{EI}V_{II}^{-1}V_{IE}V_{EE}^{-1}) \tag{2}$$

was derived, where $\rho(FV^{-1})$ was the spectral radius of FV^{-1} and

$$F = \begin{pmatrix} 0 & F_{EI} & 0 \\ 0 & 0 & 0 \\ 0 & 0 & 0 \end{pmatrix}, V = \begin{pmatrix} V_{EE} & 0 & 0 \\ V_{IE} & V_{II} & 0 \\ 0 & V_{HI} & V_{HH} \end{pmatrix}, \tag{3}$$

with

$$\begin{aligned}
 F_{EI} &= \begin{pmatrix} \lambda_1 C_{11} & \lambda_1 C_{21} & \cdots & \lambda_1 C_{K1} \\ \lambda_2 C_{12} & \lambda_2 C_{22} & \cdots & \lambda_2 C_{K2} \\ \vdots & \vdots & \ddots & \vdots \\ \lambda_K C_{1K} & \lambda_K C_{2K} & \cdots & \lambda_K C_{KK} \end{pmatrix}, V_{EE} = \begin{pmatrix} V_{EE}^{(1)} & & & \\ -\omega_1 & V_{EE}^{(2)} & & \\ & \ddots & \ddots & \\ & & -\omega_{K-1} & V_{EE}^{(K)} \end{pmatrix}, \\
 V_{II} &= \begin{pmatrix} V_{II}^{(1)} & & & \\ -\omega_1 & V_{II}^{(2)} & & \\ & \ddots & \ddots & \\ & & -\omega_{K-1} & V_{II}^{(K)} \end{pmatrix}, V_{HH} = \begin{pmatrix} V_{HH}^{(1)} & & & \\ -\omega_1 & V_{HH}^{(2)} & & \\ & \ddots & \ddots & \\ & & -\omega_{K-1} & V_{HH}^{(K)} \end{pmatrix}, \\
 V_{IE} &= -\text{diag}\{\alpha, \alpha, \dots, \alpha\}, V_{HI} = -\text{diag}\{\theta_1, \theta_2, \dots, \theta_K\}, \\
 V_{EE}^{(k)} &= \alpha + \mu + \omega_k, V_{II}^{(k)} = \gamma_{1k} + \theta_k + \mu + \omega_k, V_{HH}^{(k)} = \gamma_{2k} + \mu + \omega_k.
 \end{aligned} \tag{4}$$

The expression of basic reproduction number of age group k to age group k , R_{0k} (i.e., the average number of the infections of age group k was led by an infected of age group k) was given by

$$R_{0k} = \frac{\alpha\lambda_k C_{kk}}{(\alpha + \mu + \omega_k)(\gamma_{1k} + \theta_k + \mu + \omega_k)}, \quad k = 1, 2, \dots, K. \tag{5}$$

Further, we defined basic reproduction number of an infected of age group k to the total population, R_0^k (i.e., the average number of the infections of the local population was led by an infected of age group k) was described by

$$R_0^k = \frac{\alpha\lambda_k \sum_{j=1}^K C_{kj}}{(\alpha + \mu + \omega_k)(\gamma_{1k} + \theta_k + \mu + \omega_k)}, \quad k = 1, 2, \dots, K. \tag{6}$$

Meanwhile, we defined basic reproduction number of an infected of the total population to age group k , \hat{R}_0^k (i.e., the average number of the infections of age group k was led by an infected of the total population) was described by

$$\hat{R}_0^k = \frac{\alpha\lambda_k \sum_{j=1}^K w_j C_{jk}}{(\alpha + \mu + \omega_k)(\gamma_{1k} + \theta_k + \mu + \omega_k)}, \quad k = 1, 2, \dots, K, \tag{7}$$

where w_j denoted the probability that an infected coming from age group j of the total population.

2.5. Effective reproduction number

We collected the daily cases of the surveillance data for Fuzhou COVID-19 large wave from Fujian CDC, then used EpiEstim R package in (Cori et al., 2013; R Core Team, 2019) to estimate effective reproduction number R_t . Meanwhile, the curves of effective reproduction number for each age group were performed by using the SEIHR model, which were operated by software MATLAB. Alternatively, the precise expression of effective reproduction number from (Huang, 2008) was applied on the tendencies of COVID-19 in (Bai et al., 2023; Sun, et al., 2023; Wei et al., 2020) and Monkeypox in (Wei et al., 2022).

2.6. Sensitivity analysis

2.6.1. Local sensitivity analysis by partial derivative

According to the work in (Wei et al., 2023), we defined sensitivity index and impact magnitude of R_{0k} as follows

$$\Gamma = \Gamma(P) := \frac{\partial R_{0k}}{\partial P} \cdot \frac{P}{R_{0k}}, \quad m := \log_{10}|\Gamma|, \tag{8}$$

where P was the parameter of model (1), and was referred as to $\mu, \alpha, \omega_k, \gamma_{1k}, \lambda_k, \theta_k$ and C_{kk} .

2.6.2. Global sensitivity analysis by PRCC

The global sensitivity analysis was performed by using Latin Hypercube sampling (LHS) and Partial Rank Correlation Coefficient (PRCC) methodology in (Alvey et al., 2015; Duan & Jin, 2022; Marino et al., 2008; Taboe et al., 2022) in this study.

3. Results

3.1. Data fittings of Fuzhou COVID-19 large wave

By using of the idea of Least Squares method (i.e., the object was to minimize the differences between the numerical simulation and the surveillance data from Fujian CDC), we performed the simulations for the infected I_k in blue and the hospitalized H_k in orange in Fig. 3, according to the surveillance data, together with the initial values (Table B.1) and the parameter values (Table B.2, Table B.3) for four age groups. Further, we concerned the transmission features of G4 group in the total population. The numerical investigations against the surveillance data from Fujian CDC showed that G4 group was high-risk group in the total population, the value of effective reproduction number for G4 group took the highest value after Ten New Measures due to high susceptibility to infection and high risks on the basic diseases. While, the value of effective reproduction number for G2 group took the lowest value after Ten New Measures because schools and universities became the key regions for future surveillance spots. The research results indicated that the main parameters such as susceptibility to infection, average number of contacts, average hospitalization rates and average recovery rates for high-risk group were main options to control COVID-19 infection scale.

3.2. Estimation of basic reproduction number

By the next generation matrix method, the expression of basic reproduction number R_0 was obtained in (2). We substituted the parameter values in Table B.2 and the values of contact matrix in Fig. 2b into (2) and (4) to estimate $R_0 = 1.5718$, which implied that an infected case averagely produced 1.5718 new infection cases as offspring within the total population. By the same arguments, the values of R_{0k} were calculated as follows

$$R_{01} = 0.3135, R_{02} = 0.5427, R_{03} = 1.2019, R_{04} = 0.5136.$$

The largest value of R_{03} reflected that G3 group was the most active group in the total population. Again, by expression (6), we calculated that

$$R_0^1 = 0.8228, R_0^2 = 1.1954, R_0^3 = 1.6679, R_0^4 = 2.2469.$$

Obviously, $R_{0k} < R_0^k$ were valid for each group k , which yielded that an infected of age group k contributed less infection cases to age group k , while an infected of age group k contributed more infection cases to other three groups. By expression (7) and the probability vector $w = (0.15, 0.10, 0.50, 0.25)$ for four age groups, the calculation gave that

$$\hat{R}_0^1 = 0.1173, \hat{R}_0^2 = 0.1206, \hat{R}_0^3 = 0.9563, \hat{R}_0^4 = 0.3484.$$

Obviously, $R_{0k} > \hat{R}_0^k$ held for each group k , which implied that an infected of age group k contributed more infection cases to age group k , but, an infected of the total population contributed less infection cases to age group k . Especially, we obtained that

$$\hat{R}_0 = \hat{R}_0^1 + \hat{R}_0^2 + \hat{R}_0^3 + \hat{R}_0^4 = 1.5426,$$

which indicated that the average number of the infections by an infected of the total population reached around 1.54.

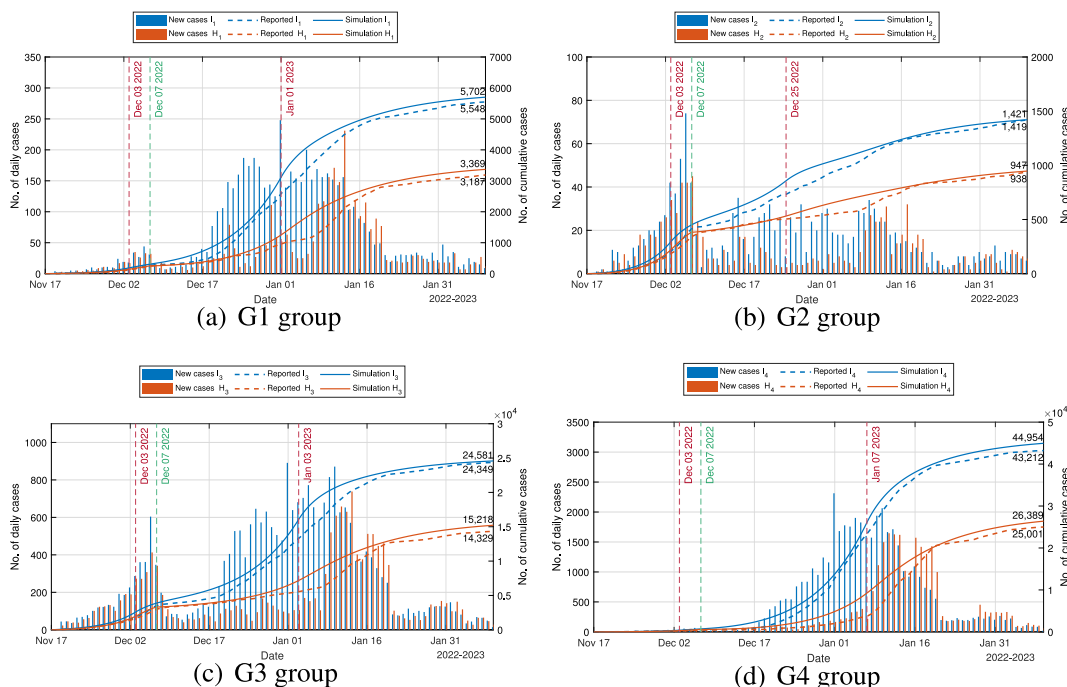


Fig. 3. The daily cases, cumulative cases and numerical simulations for four age groups of Fuzhou COVID-19 large wave. The daily cases with bars of the infected and the hospitalized came from the surveillance data of Fujian CDC. The cumulative cases in dashed curves and numerical simulations in solid curves were plotted for four age groups of Fuzhou COVID-19 large wave. The susceptibility to infection of age groups (λ_k) were changed twice starting from December 3 of the year 2022 with red dashed vertical line. The average hospitalization rates of age groups (θ_k) were changed on December 7 of the year 2022 with green dashed vertical line, which were consistent with the values and periods in Table B.3.

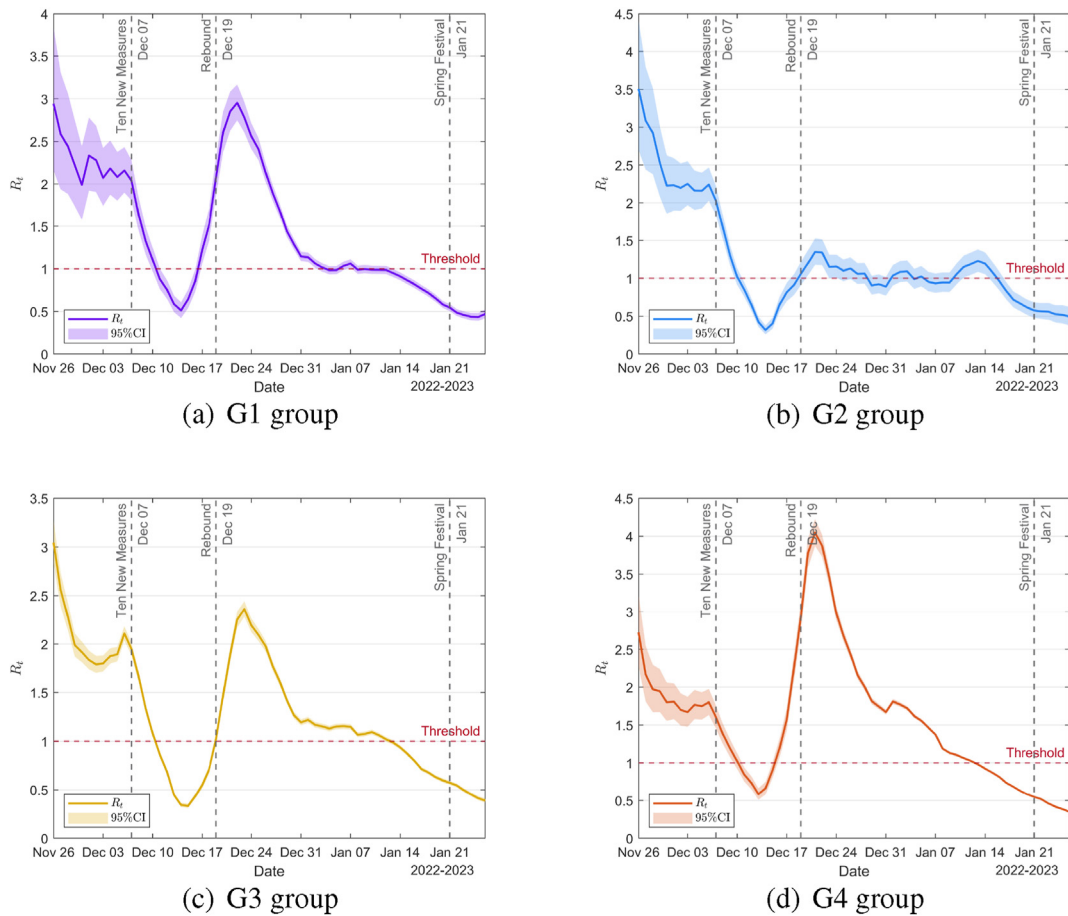


Fig. 4. Tendencies of effective reproduction number R_t for four age groups in Fuzhou COVID-19 large wave. The implements of Ten New Measures on December 7 brought the fluctuations of Fuzhou COVID-19 large wave. The rebounding tendency reached the peak after December 19 of the year 2022, Fuzhou COVID-19 large wave was controlled around January 12.

3.3. Estimation of effective reproduction number

The curve of effective reproduction number R_t reflected the evolution tendency of the average number of the infections by an infected of the total population with the time t , which was an effective indicator of a COVID-19 course in the total population at time t . The evolution tendency of R_t was run by EpiEstim R package in (Cori et al., 2013; R Core Team, 2019) and MATLAB using the surveillance data and the SEIHR model. Precisely, Fig. 4 using the surveillance data showed that the tendency curves fluctuated above threshold one during the measure operation period from November 11 to December 7 of the year 2022, Fuzhou COVID-19 large wave was controlled around January 12 of having 9 days away from Spring Festival on January 21 of the year 2023. Fig. 5 and Fig. 6 using the SEIHR model gave the similar curves for Fuzhou COVID-19 large wave, which implied that the control date was January 7 of having two weeks away from Spring Festival on January 21 of the year 2023. Here, the expression of effective reproduction number of each age group k was formulated by using the SEIHR model, which was given by

$$R_t^k = \hat{R}_0^k \times \frac{S_k(t)}{N_k(t)}. \tag{9}$$

The curves in Fig. 5 showed that effective reproduction number of G3 group was larger than other three groups, which implied that G3 group was active during the implements of Twenty Measures; both G3 group and G4 group were the main contributors of infection scale after the implements of Ten New Measures on the Chinese mainland. The curves in Fig. 5 also revealed that each age group of Fuzhou COVID-19 large wave was controlled on distinct date from December 25 to January 7 of the year 2023. By the same discussion, the expression of effective reproduction number of the total population was given by the formula

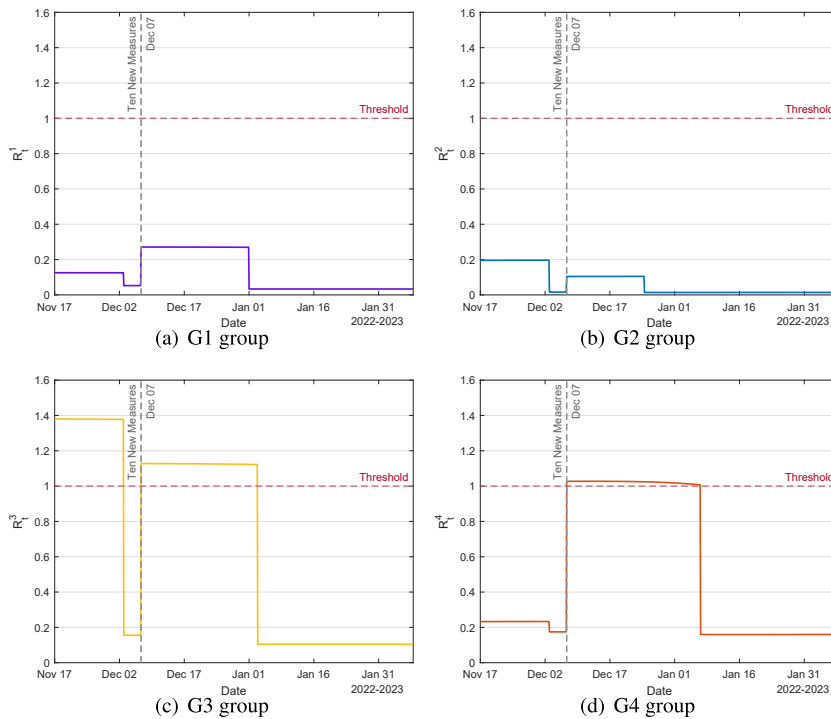


Fig. 5. The expression of R_t^k for four age groups of Fuzhou COVID-19 large wave was given by formula (9). The value of R_t^3 for G3 group took the largest value during the implements of Twenty Measures. After the implements of Ten New Measures, both G3 group and G4 group took the high thresholds, G1 group and G2 group instead. Fuzhou COVID-19 large wave was controlled on the date ranging from December 25 to January 7 for each age group.

$$R_t = R_0 \times \frac{S(t)}{N(t)}, \quad S(t) = S_1(t) + \dots + S_4(t), \tag{10}$$

where $N(t)$ is a constant. The curve of R_t in Fig. 6 fluctuated around one and kept the large value ongoing after the release of Ten New Measures until Fuzhou COVID-19 large wave was controlled.

3.4. Study of sensitivity analysis

The local sensitivity analysis with respect to the main parameters was concerned in (Yang et al., 2020) for describing the importance of each parameter. The sensitivity analysis with respect to each parameter consisted of sensitivity index and impact magnitude in (8). The top panel of Fig. 7 revealed that frequent social contacts between the susceptible and the infected led to the increments of the values of C_{kk} , and that the values of R_{0k} for each group were enlarged by formula (5),

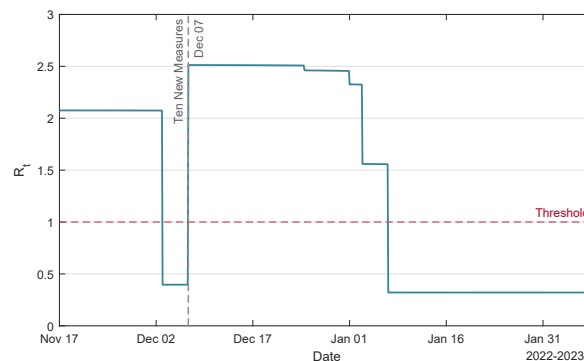


Fig. 6. The expression of R_t for the total population of Fuzhou COVID-19 large wave was given by formula (10). The threshold was above one during the implements of Twenty Measures and Ten New Measures, Fuzhou COVID-19 large wave was controlled on January 7.

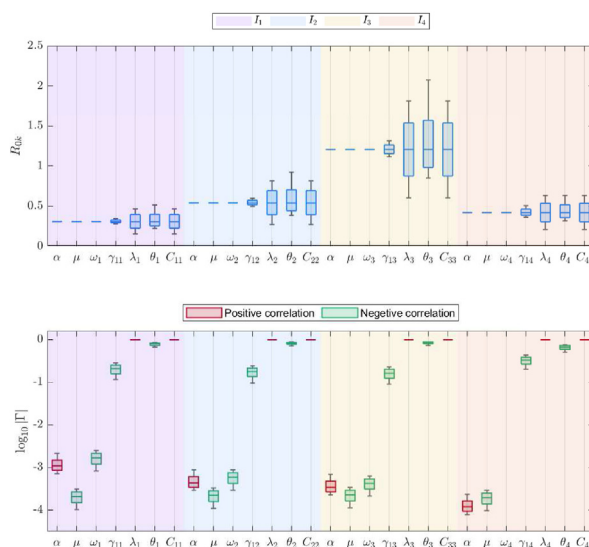


Fig. 7. Local sensitivity analysis of R_{0k} with respect to the main parameters of the SEIHR model. The parameters λ_k , C_{kk} , θ_k and γ_{1k} had significant impacts on R_{0k} , using the formula $\log_{10}|\Gamma|$ for four age groups.

which implied that infection scale of Fuzhou COVID-19 large wave for each group was increasing with the time. The bottom panel of Fig. 7 demonstrated that the main parameters λ_k , C_{kk} , θ_k and γ_{1k} had significant impacts on R_{0k} , of which λ_k and C_{kk} exhibited positive correlations, while θ_k and γ_{1k} displayed negative correlations. In other words, the impact magnitudes of average recovery rates γ_{1k} and average hospitalization rates θ_k were significant, which were beneficial for the local government to reduce COVID-19 infection scale. Further, these main parameters were usually governed to control R_{0k} and COVID-19 infection scale by implementing non-pharmaceutical interventions. Consequently, the sensitivity analysis in Fig. 7 provided the essential insights into the intervention and control strategies against COVID-19. The results of this study pointed that the public health policymakers were suggested to prepare the adequate hospital beds against future risks and medical runs.

The global sensitivity analysis was performed for understanding the impacts of the main parameters on the peak number of the infected individuals to the SEIHR model. Using the Latin Hypercube Sampling (LHS) and Partial Rank Correlation Coefficients (PRCCs) on the main parameters of Table B.2 and Fig. 2b, the global sensitivity analysis was performed when we set the sample size to be 3000. Precisely, we adopted the normal distributions for each parameter as described in (Alvey et al., 2015; Duan & Jin, 2022; Marino et al., 2008; Taboe et al., 2022), the parameter values were regarded as the mean, the standard deviation was set as 0.02 for each parameter, then the significance of PRCC values for the SEIHR model was derived in Fig. 8. The magnitude of the PRCCs reflected the sensitivity of the main parameters, the sign of the PRCCs indicated whether the relationship between the main parameters and the peak number of infections was positive (+) or negative (-).

4. Discussion and conclusion

Under the background of the implements of Twenty Measures and Ten New Measures, together with the establishment of the herd immunity by vaccination to the total population on the Chinese mainland, an SEIHR model with age groups and social contacts was built up in this study, by collecting the hospitalized cases from the surveillance data of Fujian CDC. The SEIHR model of this study enriched the existing compartment models for investigating COVID-19. First of all, we explored the epidemiological features of Fuzhou COVID-19 large wave including the expressions of basic reproduction number R_0 for the total population and for the specific age group by using of the next generation matrix method. Then, the PRCC values of sensitivity analysis showed that high-risk group became the key population contributing the hospital beds due to their high susceptibility to infection and their high risks to basic diseases. Meanwhile, the tendencies of effective reproduction number R_t were described using the surveillance data and the SEIHR model. The demonstrations in Figs. 4–Fig. 6 showed the high similarity of the tendency.

4.1. Approximation of basic reproduction number

It was obvious that the expression R_0 was dependent on each age group of the total population, the implicit expression of R_0 was derived using formula (2). While, the explicit expression \hat{R}_0 governing \hat{R}_0^k of four age groups was the approximation of basic reproduction number R_0 . We referred \hat{R}_0 as the age-weighting basic reproduction number due to the appearance of the probability vector $w = (w_1, w_2, w_3, w_4)$ in this study, which reflected the average number of the infections of age groups (i.e.,

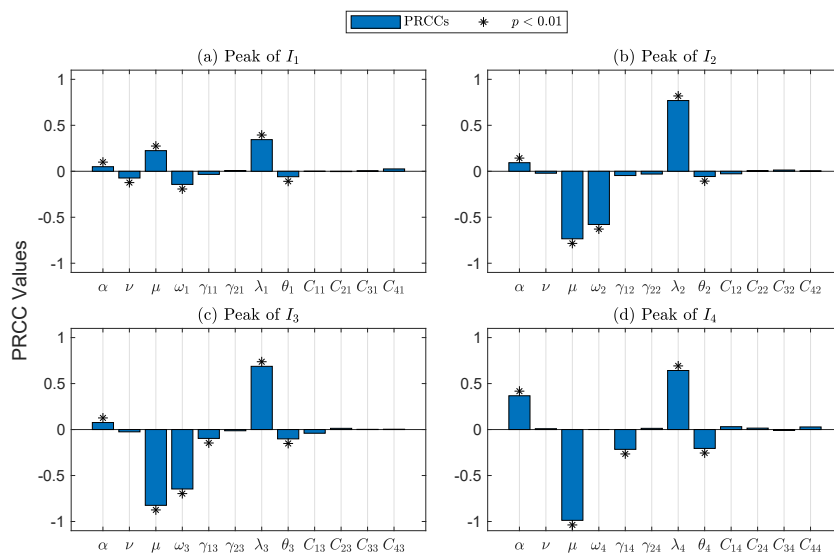


Fig. 8. Global sensitivity analysis: PRCC values for the peak numbers of the infected of four age groups. The sample size was set to be 3000. Parameter values and the values in contact matrix were provided in Table B.2 and Fig. 2b. (*) denoted that the PRCCs were significant (p -value < 0.01), among which the susceptibility to infection (λ_k), the incubation period ($1/\alpha$) and aging rate (ω_k) of four age groups were significant.

G1 group to G4 group) led by an infected of the total population. Under the real circumstances, the epidemiological meaning of \hat{R}_0 admitted the similar meaning with basic reproduction number R_0 , the computation of \hat{R}_0 was easily handled than that of basic reproduction number R_0 .

4.2. Scenarios investigations

We assumed that the mutation of SARS-CoV-2 variants was kept very small, and that contact matrix C of four age groups in Fig. 2 was regarded as basic scenario in this section. The distributions of infection cases in Fig. 3 and the tendencies of R_t in Fig. 3 revealed that hospitalized cases in G4 group took the largest infection scale during Fuzhou COVID-19 large wave. So, we chose G4 group for further scenario investigations with fixed values in Table B.2 and Table B.3, changing the coefficient of contact matrix C . The results showed that changes of social contact patterns of the total population led to the variations of severe infections in Fig. 9.

4.3. Added value of this study

The main results of this study showed that susceptibility to infection (λ_k) of G4 group was the highest by data fittings, and also that susceptibility to infection (λ_k) were significant on the spread of COVID-19 by using PRCC values. Meanwhile, the differences of the tendencies of effective reproduction number R_t^k by using the surveillance data and the SEIHR model varied with age group. As a consequence, high-risk group (i.e., G4 group) became the key population because it contributed the majority of hospital beds after the implements of Ten New Measures. The comprehensive investigations regarding the hospital-beds requirements and age groups of the total population revealed that high-risk group should be paid more attention on their hospital beds and medicine supply during the global circulation of COVID-19.

4.4. Implications of all the available evidence

This study presented the differences and social contacts of age groups against COVID-19, which provided the important insights for policymakers. The hospital-bed indicator was an effective approach for studying COVID-19 new variant after Twenty Measure on the Chinese mainland. This study presented the differences of social contacts among age groups against COVID-19, which provided the important insights for policymakers. The heterogeneities of age groups and contact matrix were kept for the relative analyses of basic reproduction number, effective reproduction number and the sensitivity analysis. The multi-age groups SEIHR model was applied to other cities/regions by governing the liable surveillance data from the CDC when the duration of COVID-19 was short. The situation of hospital-bed requirements was an effective approach for studying COVID-19 new variant after Ten New Measures on the Chinese mainland.

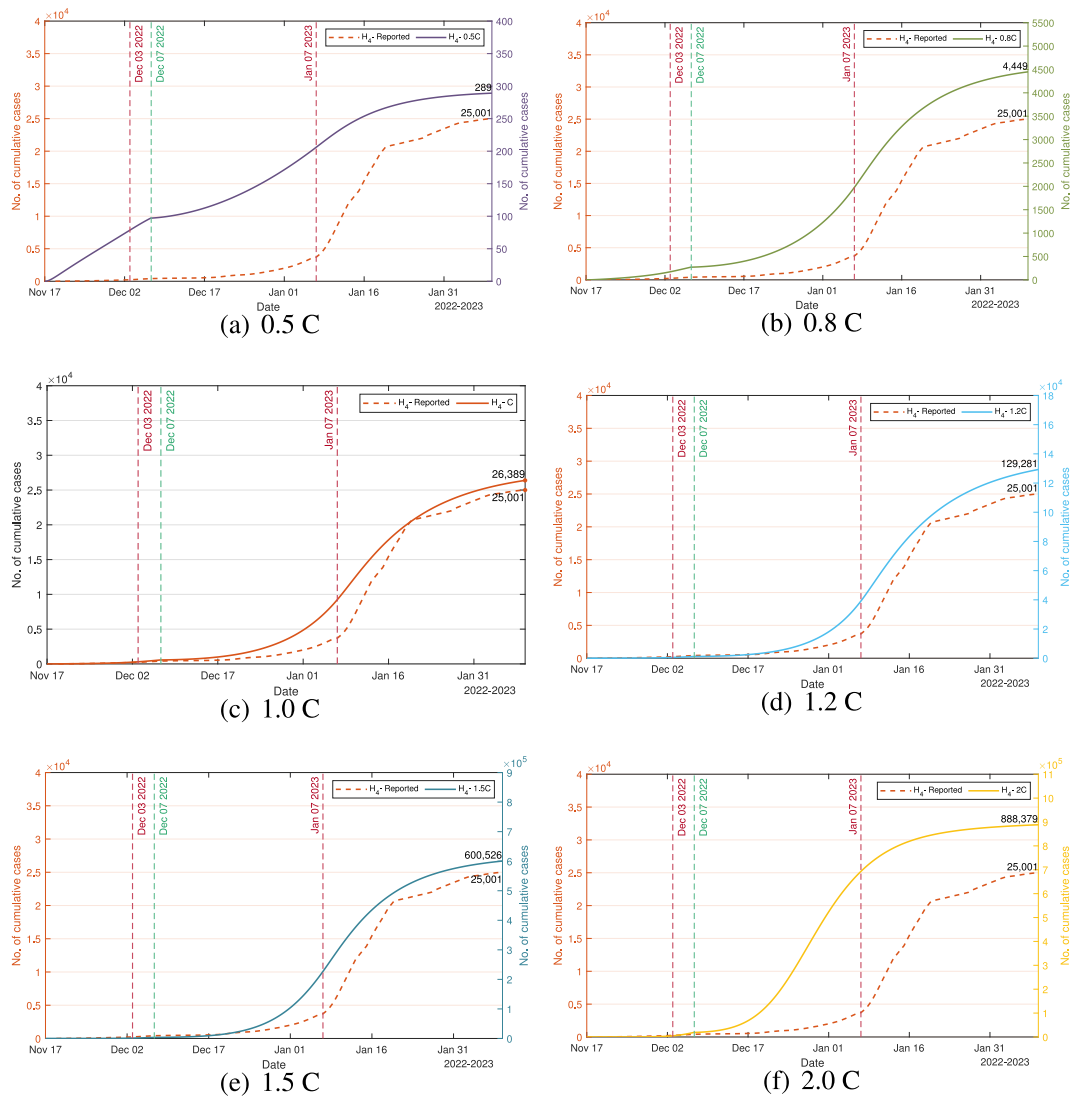


Fig. 9. Scale scenario investigations for the hospitalized cases in G4 group. The surveillance data of the hospitalized for G4 group were from Fujian CDC in dashed curves on the left axis. The scale scenario simulations of the hospitalized for G4 group were in solid curves as presented on the right axis. The switchings for the susceptibility to infection (λ_4) in red dashed vertical line and the average hospitalization rates (θ_4) in green dashed vertical line were kept same with those of G4 group in Fig. 8 and Table B.3.

4.5. Limitations of this study

Throughout this study, the migration of age groups of the total population in Fuzhou City was not considered due to the short duration of Fuzhou COVID-19 large wave; the appearance and the prevalence of SARS-CoV-2 new variant was not included because the domination of SARS-CoV-2 Omicron variant lasted over six months on the Chinese mainland.

Ethics approval and consent to participate

The ethical approval and individual consents were exempted as the aggregated data were used in this study.

Funding

This study received the supports from Special Projects of the Central Government Guiding Local Science and Technology Development (2021L3018), Natural Science Foundation of Fujian Province of China (2021J01621), and Consultancy Project by

the Chinese Academy of Engineering (2022-JB-06), National Natural Science Foundation of China (12231012), Royal Society of Edinburgh (RSE1832) and Engineering and Physical Sciences Research Council (EP/W522521/1).

Data and material availability

The data that supported this article may be available upon reasonable request to the corresponding author.

CRediT authorship contribution statement

Xiaomin Lan: Writing – original draft, Software, Formal analysis, Data curation. **Guangmin Chen:** Data curation. **Ruiyang Zhou:** Visualization. **Kuicheng Zheng:** Writing – review & editing, Methodology. **Shaojian Cai:** Resources, Data curation. **Fengying Wei:** Writing – review & editing, Supervision, Project administration, Methodology. **Zhen Jin:** Supervision, Project administration, Conceptualization. **Xuerong Mao:** Supervision, Project administration, Methodology.

Declaration of competing interest

The authors declare that they have no known competing financial interests or personal relationships that could have appeared to influence the work reported in this paper.

Acknowledgements

FYW was supported by Special Projects of the Central Government Guiding Local Science and Technology Development (2021L3018), Natural Science Foundation of Fujian Province of China (2021J01621), and Consultancy Project by the Chinese Academy of Engineering (2022-JB-06), ZJ was supported by National Natural Science Foundation of China (12231012), XRM was supported by Royal Society of Edinburgh (RSE1832) and Engineering and Physical Sciences Research Council (EP/W522521/1).

Appendix A. The computation of the elements in 4 × 4 contact matrix

Let $C_{[j_1-j_2] \rightarrow [k_1-k_2]}$ be the element of the 16×16 contact matrix, where $[j_1 - j_2]$ or $[k_1 - k_2]$ stands for one of age groups $[0 - 4]$, $[5 - 9]$, ..., $[70 - 74]$, $[75 +]$. We supposed that $C_{[j_1-j_2] \rightarrow [k_1-k_2]}$ is the daily average number of contacts with the individuals of age group $[k_1 - k_2]$ by an individual of age group $[j_1 - j_2]$, $C_{[j] \rightarrow [k_1-k_2]}$ is the daily average number of contacts with the individuals of age group $[k_1 - k_2]$ by an individual of age $[j]$, $C_{[j_1-j_2] \rightarrow [k]}$ is the daily average number of contacts with the individuals of age $[k]$ by an individual of age group $[j_1 - j_2]$. Further, for $j \in [j_1 - j_2]$, $k \in [k_1 - k_2]$, we supposed that $C_{[j] \rightarrow [k_1-k_2]} = C_{[j_1-j_2] \rightarrow [k_1-k_2]}$ and $C_{[j_1-j_2] \rightarrow [k]} = \frac{1}{5}C_{[j_1-j_2] \rightarrow [k_1-k_2]}$ held in this study. For example, the daily average number of contacts with the individuals of age group $[0 - 11]$ by an individual of age group $[0 - 11]$ was calculated as follows:

$$\begin{aligned}
 C_{[0-11] \rightarrow [0-11]} &= \sum_{j=0}^4 \frac{1}{12}C_{[j] \rightarrow [0-11]} + \sum_{j=5}^9 \frac{1}{12}C_{[j] \rightarrow [0-11]} + \sum_{j=10}^{11} \frac{1}{12}C_{[j] \rightarrow [0-11]} \\
 &= \frac{5}{12}C_{[0-4] \rightarrow [0-11]} + \frac{5}{12}C_{[5-9] \rightarrow [0-11]} + \frac{2}{12}C_{[10-14] \rightarrow [0-11]} \\
 &= \frac{5}{12} \left(C_{[0-4] \rightarrow [0-4]} + C_{[0-4] \rightarrow [5-9]} + C_{[0-4] \rightarrow [10-11]} \right) \\
 &+ \frac{5}{12} \left(C_{[5-9] \rightarrow [0-4]} + C_{[5-9] \rightarrow [5-9]} + C_{[5-9] \rightarrow [10-11]} \right) \\
 &+ \frac{2}{12} \left(C_{[10-14] \rightarrow [0-4]} + C_{[10-14] \rightarrow [5-9]} + C_{[10-14] \rightarrow [10-11]} \right) \\
 &= \frac{5}{12} \left(C_{[0-4] \rightarrow [0-4]} + C_{[0-4] \rightarrow [5-9]} + \frac{2}{5}C_{[0-4] \rightarrow [10-14]} \right) \\
 &+ \frac{5}{12} \left(C_{[5-9] \rightarrow [0-4]} + C_{[5-9] \rightarrow [5-9]} + \frac{2}{5}C_{[5-9] \rightarrow [10-14]} \right) \\
 &+ \frac{2}{12} \left(C_{[10-14] \rightarrow [0-4]} + C_{[10-14] \rightarrow [5-9]} + \frac{2}{5}C_{[10-14] \rightarrow [10-14]} \right)
 \end{aligned}$$

In fact, $C_{[0-11] \rightarrow [0-11]}$ was C_{11} .

Appendix B. Four main tables to model (1)

Table B.1

Initial values of Fuzhou COVID-19 large wave

Variable	$k = 1$	$k = 2$	$k = 3$	$k = 4$	Source
$S_k(0)$	1,147,146	728,097	5,024,766	1,389,545	Calculated ^a
$E_k(0)$	16	8	175	32	FHC ^b
$I_k(0)$	0	0	0	0	Assumed
$H_k(0)$	0	0	0	0	Assumed
$R_k(0)$	270	340	560	430	FHC ^c
$N_k(0)$	1,147,424	728,441	5,025,414	1,389,989	FSB ^d

^a $S_k(0)$ were calculated by $S_k(0) = N_k(0) - E_k(0) - I_k(0) - H_k(0) - R_k(0)$.

^b FHC was Fuzhou Health Commission in (Fuzhou Health Commission, 2023), and FSB was Fuzhou Statistic Bureau in (Fuzhou Statistics Bureau, 2020).

Table B.2

Main parameter values of Fuzhou COVID-19 large wave

Para.	$k = 1$	$k = 2$	$k = 3$	$k = 4$	Source
ΔT^a	2	2	2	2	Assumed
λ_k	0.018	0.018	0.032	0.075	Fitted ^b
ω_k	2.400×10^{-4}	8.000×10^{-5}	5.576×10^{-5}	0	(Duan & Jin, 2022)
γ_{1k}	0.070	0.053	0.045	0.058	(Huo et al., 2023)
γ_{2k}	0.41	0.48	0.36	0.26	Data ^d
θ_k	0.270	0.244	0.232	0.260	Fitted ^b
μ	2.973×10^{-5}	2.973×10^{-5}	2.973×10^{-5}	2.973×10^{-5}	FHC ^c
$1/\nu$	160	160	160	160	(Nguyen et al., 2021)
$1/\alpha$	4	4	4	4	(Xiong et al., 2023)

^a ΔT denoted awareness delay in (Huang et al., 2020), referring as the period or the delay between the date of the first infection and the date of the first confirmation, unit for ΔT , $1/\nu$, $1/\alpha$ was day, unit for other parameters was day⁻¹.

^b Parameters λ_k and θ_k were average values in Table B.3, which were derived by data fittings.

^c By (Duan & Jin, 2022), the formula of ω_k were written as $\omega_k = \left(\frac{1}{MA_k - MA_{k-1}} - \frac{1}{ALS} \right) \times \frac{1}{365}$, where MA_k was mean age in age group k , and ALS (average life span) was 80.41 years old in (Fuzhou Statistics Bureau, 2020).

^d Parameters $1/\gamma_{2k}$ were calculated as the average length of hospitalization spent for each age group by surveillance data from Fujian CDC.

^e FHC was Fuzhou Health Commission in (Fuzhou Health Commission, 2023).

Table B.3

Estimations for λ_k and θ_k

Para.	Period	Value	Para.	Period	Value
λ_1	Nov 19, 2022–Dec 03, 2022	0.050	λ_2	Nov 19, 2022–Dec 03, 2022	0.080
	Dec 04, 2022–Jan 01, 2023	0.021		Dec 04, 2022–Dec 25, 2022	0.0065
	Jan 02, 2023–Feb 09, 2023	0.0026		Dec 26, 2022–Feb 09, 2023	0.00085
	Average in time ^a	0.0181		Average in time ^a	0.0176
	<hr/>				<hr/>
λ_3	Nov 19, 2022–Dec 03, 2022	0.133	λ_4	Nov 19, 2022–Dec 03, 2022	0.135
	Dec 04, 2022–Jan 03, 2023	0.015		Dec 04, 2022–Jan 07, 2023	0.101
	Jan 04, 2023–Feb 09, 2023	0.0014		Jan 08, 2023–Feb 09, 2023	0.016
	Average in time ^a	0.0318		Average in time ^a	0.0747
	<hr/>				<hr/>
θ_1	Nov 19, 2022–Dec 07, 2022	0.8075	θ_2	Nov 19, 2022–Dec 07, 2022	0.7614
	Dec 08, 2022–Feb 09, 2023	0.100		Dec 08, 2022–Feb 09, 2023	0.072
	Average in time ^a	0.270		Average in time ^a	0.238
<hr/>			<hr/>		
θ_3	Nov 19, 2022–Dec 07, 2022	0.757	θ_4	Nov 19, 2022–Dec 07, 2022	0.803
	Dec 08, 2022–Feb 09, 2023	0.065		Dec 08, 2022–Feb 09, 2023	0.088
	Average in time ^a	0.232		Average in time ^a	0.260

^a Average in time = $(P_1 \times V_1 + P_2 \times V_2 + P_3 \times V_3)/(P_1 + P_2 + P_3)$, where P_i and V_i are the periods and the values that parameters belong to.

References

- Alvey, C., Feng, Z., & Glasser, J. (2015). A model for the coupled disease dynamics of HIV and HSV-2 with mixing among and between genders. *Mathematical Biosciences*, 265, 82–100. <https://doi.org/10.1016/j.mbs.2015.04.009>
- Bai, Y., Peng, Z., Wei, F., Jin, Z., Wang, J., Xu, X., et al. (2023). Study on the COVID-19 epidemic in mainland China between november 2022 and january 2023, with prediction of its tendency. *Journal of Biosafety and Biosecurity*, 5(1), 39–44. <https://doi.org/10.1016/j.job.2023.03.001>
- Chen, Z., Deng, X., Fang, L., Sun, K., Wu, Y., Che, T., et al. (2022). Epidemiological characteristics and transmission dynamics of the outbreak caused by the SARS-CoV-2 omicron variant in Shanghai, China: A descriptive study. *The Lancet Regional Health - Western Pacific*, 29, Article 100592. <https://doi.org/10.1016/j.lanwpc.2022.100592>
- Cori, A., Ferguson, N. M., Fraser, C., & Cauchemez, S. (2013). A new framework and software to estimate time-varying reproduction numbers during epidemics. *American Journal of Epidemiology*, 178(9), 1505–1512. <https://doi.org/10.1093/aje/kwt133>
- Duan, M., & Jin, Z. (2022). The heterogeneous mixing model of COVID-19 with interventions. *Journal of Theoretical Biology*, 553, Article 111258. <https://doi.org/10.1016/j.jtbi.2022.111258>
- Fuzhou Health Commission. (2023). *Fuzhou health commission*. Retrieved from <https://www.fuzhou.gov.cn/zfgzft/swjw/fzwj/>. (Accessed 15 March 2024).
- Fuzhou Statistics Bureau. (2020). *Fuzhou Statistics Bureau*. Retrieved from <http://tjj.fuzhou.gov.cn/>. (Accessed 15 March 2024).
- Health Commission of Fujian Province. (2022a). *Vaccination situation for SARS-CoV-2 of fujian Province*. Retrieved from https://wjw.fujian.gov.cn/ztzl/gzbufk/yqtb/202211/t20221102_6032311.htm. (Accessed 15 March 2024).
- Health Commission of Fujian Province. (2022b). *Vaccination situation for SARS-CoV-2 of fujian Province*. Retrieved from https://wjw.fujian.gov.cn/ztzl/gzbufk/yqtb/202212/t20221221_6082224.htm. (Accessed 15 March 2024).
- Huang, S. (2008). A new SEIR epidemic model with applications to the theory of eradication and control of diseases, and to the calculation of R_0 . *Mathematical Biosciences*, 215(1), 84–104. <https://doi.org/10.1016/j.mbs.2008.06.005>
- Huang, S., Wei, F., Peng, Z., Jin, Z., Wang, J., Xu, X., et al. (2020). Assessment method of coronavirus disease 2019 outbreaks under normal prevention and control. *Disease Surveillance*, 35(8), 679–686. <https://doi.org/10.3784/j.issn.1003-9961.2020.08.004>
- Huo, D., Yu, T., Shen, Y., Pan, Y., Li, F., Cui, S., et al. (2023). A comparison of clinical characteristics of infections with SARS-CoV-2 Omicron subvariants BF.7.14 and BA.5.2.48 — October-December 2022. *China CDC Weekly*, 5(23), 511–515. <https://doi.org/10.46234/ccdcw2023.096>
- Kimathi, M., Mwalili, S., Ojiambo, V., & Gathungu, D. K. (2021). Age-structured model for COVID-19: Effectiveness of social distancing and contact reduction. *Infectious Disease Modelling*, 6, 15–23. <https://doi.org/10.1016/j.idm.2020.10.012>
- Lan, X., Chen, G., Zhou, R., Zheng, K., Cai, S., & Wei, F., et al. (2024). Dynamics of a stochastic epidemic model with age-group. *Mathematica Applicata*. (Accessed 28 March 2024).
- Li, D., Wei, F., & Mao, X. (2022). Stationary distribution and density function of a stochastic SVIR epidemic model. *Journal of the Franklin Institute-Engineering and Applied Mathematics*, 359(16), 9422–9449. <https://doi.org/10.1016/j.jfranklin.2022.09.026>
- Liang, W., Liu, M., Liu, J., Wang, Y. D., Wu, J., & Liu, X. (2022). The dynamic COVID-zero strategy on prevention and control of COVID-19 in China. *National Medical Journal of China*, 102(4), 239–242. <https://doi.org/10.3760/cma.j.cn112137-20211205-02710>
- Liu, F., & Wei, F. (2022). An epidemic model with Beddington-DeAngelis functional response and environmental fluctuations. *Physica A: Statistical Mechanics and its Applications*, 597, Article 127321. <https://doi.org/10.1016/j.physa.2022.127321>
- Lu, R., & Wei, F. (2019). Persistence and extinction for an age-structured stochastic SVIR epidemic model with generalized nonlinear incidence rate. *Physica A: Statistical Mechanics and its Applications*, 513, 572–587. <https://doi.org/10.1016/j.physa.2018.09.016>
- Makhoul, M., Chemaitelly, H., Ayoub, H., Seedat, S., & Abu-Raddad, L. (2021). Epidemiological differences in the impact of COVID-19 vaccination in the United States and China. *Vaccines*, 9(3), 223. <https://doi.org/10.3390/vaccines9030223>
- Marino, S., Hogue, I. B., Ray, C. J., & Kirschner, D. E. (2008). A methodology for performing global uncertainty and sensitivity analysis in systems biology. *Journal of Theoretical Biology*, 254(1), 178–196. <https://doi.org/10.1016/j.jtbi.2008.04.011>
- Nguyen, N. N., Houhamdi, L., Delorme, L., Colson, P., & Gautret, P. (2021). Reinfections with different SARS-CoV-2 Omicron subvariants, France. *Emerging Infectious Diseases*, 28(11), 2341–2343. <https://doi.org/10.3201/eid2811.221109>
- People's Daily Online. (2023). *Mainland China finished the full vaccination for 1272.83 million individuals as of November 28 of the year 2023*. Retrieved from <http://health.people.com.cn/n1/2022/1129/c14739-32576966.html>. (Accessed 15 March 2024).
- Prem, K., Zandvoort, K. V., Klepac, P., Eggo, R. M., Davies, N. G., Cook, A. R., et al. (2021). Projecting contact matrices in 177 geographical regions: An update and comparison with empirical data for the COVID-19 era. *PLoS Computational Biology*, 17(7), Article e1009098. <https://doi.org/10.1371/journal.pcbi.1009098>
- R Core Team. (2019). *R: A language and environment for statistical computing*. Vienna, Austria: R Foundation for Statistical Computing. <https://www.r-project.org/>.
- Sun, Y., Wang, M., Wei, F., Huang, S., & Xu, J. (2023). COVID's future: Viral multi-lineage evolution and the dynamics of small epidemic waves without seasonality in COVID-19. *Journal of Biosafety and Biosecurity*, 5(3), 96–99. <https://doi.org/10.1016/j.job.2023.07.003>
- Taboe, H. B., Asare-Baah, M., Yesmin, A., & Ngonghala, C. N. (2022). The impact of age structure and vaccine prioritization on COVID-19 in West Africa. *Infectious Disease Modelling*, 7(4), 709–727. <https://doi.org/10.1016/j.idm.2022.08.006>
- Tan, Z., Chen, Z., Yu, A., Li, X., Feng, Y., Zhao, X., et al. (2022). The first two imported cases of SARS-CoV-2 Omicron variant — Tianjin Municipality, China, December 13, 2021. *China CDC Weekly*, 4(4), 76–77. <https://doi.org/10.46234/ccdcw2021.266>
- Ten New Measures. (2022). *The State Council joint prevention and control mechanism against COVID-19*. Retrieved from https://www.gov.cn/xinwen/2022-12/07/content_5730443.htm. (Accessed 15 March 2024).
- The State Council The People's Republic of China. (2022a). *China releases measures to optimize COVID-19 response*. Retrieved from https://english.www.gov.cn/news/topnews/202211/11/content_WS636e31efc6d0a757729e2e63.html. (Accessed 15 March 2024).
- The State Council The People's Republic of China. (2022b). *COVID-19 response further optimized with 10 new measures*. Retrieved from https://english.www.gov.cn/statecouncil/ministries/202212/08/content_WS63913c92c6d0a757729e4135.html. (Accessed 15 March 2024).
- Twenty Measures. (2022). *The State Council joint prevention and control mechanism against COVID-19*. Retrieved from https://www.gov.cn/xinwen/2022-11/11/content_5726144.htm. (Accessed 15 March 2024).
- van den Driessche, P., & Watmough, J. (2002). Reproduction numbers and sub-threshold endemic equilibria for compartmental models of disease transmission. *Mathematical Biosciences*, 180(1–2), 29–48. [https://doi.org/10.1016/s0025-5564\(02\)00108-6](https://doi.org/10.1016/s0025-5564(02)00108-6)
- Wei, F., Jiang, H., & Zhu, Q. (2021). Dynamical behaviors of a heroin population model with standard incidence rates between distinct patches. *Journal of the Franklin Institute-Engineering and Applied Mathematics*, 358(9), 4994–5013. <https://doi.org/10.1016/j.jfranklin.2021.04.024>
- Wei, F., Peng, Z., Jin, Z., Wang, J., Xu, X., Zhang, X., et al. (2022). Study and prediction of the 2022 global monkeypox epidemic. *Journal of Biosafety and Biosecurity*, 4(2), 158–162. <https://doi.org/10.1016/j.job.2022.12.001>
- Wei, F., Wang, J., Xu, X., Gao, J., Wang, B., Ma, C., et al. (2020). Tendency prediction of COVID-19 worldwide. *Disease Surveillance*, 35(6), 467–472. <https://doi.org/10.3784/j.issn.1003-9961.2020.06.004>
- Wei, F., & Xue, R. (2020). Stability and extinction of SEIR epidemic models with generalized nonlinear incidence. *Mathematics and Computers in Simulation*, 170, 1–15. <https://doi.org/10.1016/j.matcom.2018.09.029>
- Wei, F., Zhou, R., Jin, Z., Huang, S., Peng, Z., Wang, J., et al. (2023). COVID-19 transmission driven by age-group mathematical model in Shijiazhuang City of China. *Infectious Disease Modelling*, 8(4), 1050–1062. <https://doi.org/10.1016/j.idm.2023.08.004>
- Wu, P., & Feng, Z. (2024). Global dynamics of a space-age structured covid-19 model coupling within-host infection and between-host transmission. *Communications in Nonlinear Science and Numerical Simulation*, 131, Article 107801. <https://doi.org/10.1016/j.cnsns.2023.107801>

- Xiong, W., Peng, L., Tsang, T., & Cowling, B. (2023). Epidemiology of SARS-CoV-2 omicron BA.5 infections, Macau, June–July 2022. *Emerging Infectious Diseases*, 29(2), 453–456. <https://doi.org/10.3201/eid2902.221243>
- Yang, J., Wang, G., Zhang, S., Xu, F., & Li, X. (2020). Analysis of the age-structured epidemiological characteristics of SARS-CoV-2 transmission in Mainland China: An aggregated approach. *Mathematical Modelling of Natural Phenomena*, 15, 39–53. <https://doi.org/10.1051/mmnp/2020032>
- Yu, B., Li, Q., Chen, J., & He, D. (2023). The impact of COVID-19 vaccination campaign in Hong Kong SAR China and Singapore. *Infectious Disease Modelling*, 8(1), 101–106. <https://doi.org/10.1016/j.idm.2022.12.004>
- Zeng, T., Teng, Z., Rifhat, R., Wang, X., Wang, L., & Wang, K. (2023). Analysis and simulation of a stochastic COVID-19 model with large-scale nucleic acid detection and isolation measures: A case study of the outbreak in Urumqi, China in August 2022. *Infectious Disease Modelling*, 8(2), 356–373. <https://doi.org/10.1016/j.idm.2023.03.004>
- Zhai, X., Li, W., Wei, F., & Mao, X. (2023). Dynamics of an HIV/AIDS transmission model with protection awareness and fluctuations. *Chaos, Solitons & Fractals*, 169, Article 113224. <https://doi.org/10.1016/j.chaos.2023.113224>
- Zhang, J., & Wei, F. (2020). Effects of media coverage and temporary immunity to a stochastic SEIR epidemic model. *Annals of Applied Mathematics*, 36, 442–458.
- Zhong, H., Wang, K., & Wang, W. (2022). Spatiotemporal pattern recognition and dynamical analysis of COVID-19 in Shanghai, China. *Journal of Theoretical Biology*, 554, Article 111279. <https://doi.org/10.1016/j.jtbi.2022.111279>
- Zhou, L., Wang, Y., Xiao, Y., & Li, M. (2019). Global dynamics of a discrete age-structured SIR epidemic model with applications to measles vaccination strategies. *Mathematical Biosciences*, 308, 27–37. <https://doi.org/10.1016/j.mbs.2018.12.003>
- Zhou, R., Cai, S., Chen, G., Huang, S., Jin, Z., Peng, Z., et al. (2024). Dynamic evolution characteristics of SVEIR model with variants and non-pharmaceutical interventions for controlling COVID-19. *Journal of Biosafety and Biosecurity*. <https://doi.org/10.1016/j.jobbb.2024.02.002>. Available online 15 April 2024.